H_2 Production from the Radiolysis of Aqueous Suspensions of ZnO Nanoparticles by 5.5 MeV He^{2+} ions

Jamie S. Southworth [a,b], *Simon M. Pimblott* [a,b,c], *Sven P. K. Koehler* [b,d*]

[a] School of Chemistry, The University of Manchester, Oxford Road, Manchester, M13 9PL, UK

[b] Dalton Cumbrian Facility, The University of Manchester, Westlakes Science & Technology Park, Moor Row, CA24 3HA, UK

[c] Idaho National Laboratory, Nuclear Science User Facilities, 995 University Boulevard, Idaho Falls, ID 83401-0355, USA

[d] Fakultät II, Hochschule Hannover, Ricklinger Stadtweg 120, 30459 Hannover, Germany

[*] Corresponding author: s.koehler@mmu.ac.uk

Abstract

The effects of ion beam irradiation on aqueous suspensions of metal oxides has received relatively little attention compared to γ-ray irradiation despite being a highly prevalent process in spent nuclear fuel storage and reprocessing. This is partly due to the difficulties associated with homogeneously irradiating condensed-phase matter using α-particles. Here, we report experimental yields of H_2 from the 5.5 MeV He^{2+} ion irradiation of aqueous suspensions of ZnO nanoparticles. The obtained results are compared to our previously measured results for the γ-radiolysis of the same system. The amount of H_2 increases linearly with adsorbed dose for all studied concentrations. The measured yields are of the same order of magnitude as those observed for pure water, but decrease with increasing water content. Overall, the yields follow a similar trend to those observed for γ-ray radiolysis.

1. Introduction

The γ-ray radiolysis of water adsorbed on metal oxide surfaces has been the subject of intense study in recent years.[1,2,3,4,5,6,7] However, α-particle irradiation of these systems has received far less attention despite it being a prevalent process in storage of spent and reprocessed nuclear fuel.

The yields of the stable products formed from the γ-radiolysis of water (mainly H_2 and H_2O_2) have been investigated for many years.[8,9] However, product yields differ depending on the Linear Energy Transfer (LET = -dE/dx) of the interacting radiation.[10] As the LET of the radiation traversing an aqueous solution or suspension increases, the molecular yields of the radiolysis products increase. Thus as the LET of radiation increases, the number of ionisation and excitation events per unit distance increases. In turn, this increases the likelihood of recombination of radical species in the spurs, leading to an increased yield of molecular products.[11,12] Due to the different LET, heavy ion irradiation will result in significantly different H_2 yields than γ-rays. In high LET irradiation such as α-particle irradiation, there is a much higher local concentration of reactive species in the irradiated sample. This in turn increases the probability of second order reactions in the ion tracks, hence further processes occur before the primary species diffuse away into the bulk.[13] It is also well documented that primary ion yields are much higher compared to excited state or radical yields from high LET irradiation.[14,15]

The presence of a solid surface, however, in contact with water during radiolysis can have a profound effect upon the radiolytic yields of stable species.[16,17] Enhanced yields of H_2 are postulated to be due to efficient energy transfer from the oxide to the water.[18] This is thought to be caused by the formation and migration of excitons (electrostatically bound electron-hole pairs) from the oxide particles into the surrounding water molecules, followed by their subsequent recombination.[2] However, this is not a universally accepted mechanism. It is also documented that secondary electrons, even at energies below 20 eV, can cause dissociation of water molecules by processes such as dissociative electron attachment.[19,20] Increased yields of H_2 could lead to the formation of flammable atmospheres in high level waste storage or alteration of reactor water chemistry in

operational power stations. Hence, the interaction of radiation with aqueous suspensions or slurries of metal oxides requires thorough understanding and quantification.

Zinc oxide is a semi-conductor with band gap of ~3.3 eV. Zn cations (sometimes from depleted ZnO)[21] are injected into the primary circuit of Light Water Reactors.[22] The aim is to inhibit the incorporation of γ-ray emitting 60-Co into the pipe work by instead incorporating Zn into the pipes out of the reactor core. Thus, the addition of Zn cations would reduce 60-Co incorporation and lead to reduced radiation fields away from the reactor, decreasing the dose workers are exposed to.[23,24,25]

γ-ray radiolysis of water adsorbed on ZnO powder shows an enhancement in the yields of H_2 by an order of magnitude compared to that of pure water radiolysis, and as the water loading on the ZnO increases, the radiolytic yield of H_2 decreases. Interestingly, the production of O_2 in comparable volumes to H_2 during γ-radiolysis of water adsorbed to the surface of ZnO was also observed.[26] This is of significance as in similar experiments with other oxides, O_2 was either not observed nor detected.[4] Indeed, it is worth investigating the effect the presence of ZnO has upon the α-irradiation of water and the identity and quantity of gaseous products.

Two key radicals formed from water splitting are H and OH, and the formation of H_2 occurs when two H atoms combine. The proximity of their formation depends on the LET of the incident radiation, hence the energy deposition rate is a key parameter in determining radiolytic yields. The rate constants for reactions involving H atoms and OH radicals are significantly greater than the diffusion rate as they are highly reactive species, hence it is likely that they will react with each other before they are able to diffuse away and react with the bulk.

If spurs are formed with significant spatial separation, the most likely reaction would between the H atom and the OH radical which would reform water. This is more commonly the case with low LET radiation such as γ-rays, hence the $G(H_2)$ value of 0.22 molecules/100 eV for pure, deaerated water with no radical scavenger. As spurs are formed closer in proximity to one another, such as the case for He^{2+} particles, the likelihood of two H atoms meeting increases, hence the probability of the H_2 forming reaction increases.

The addition of a radical scavenger to water irradiated by high LET radiation does not have as profound an effect as for low LET radiation. The rate of radical reactions is so high that the H atoms are likely to react in the spur before they are able to diffuse out into the bulk and interact with a scavenger species. $G(H_2)$ is approximately ~1.20 molecules/100 eV and does not change significantly with the addition of a radical scavenger.

We describe here the 5.5 MeV He^{2+} ion irradiation of aqueous suspensions of water and ZnO. The gases produced were quantified by Gas Chromatography (GC) and the dependence of the radiation dose upon the H_2 yield was investigated, as was the variation of H_2 as a function of the weight percent (wt%) of water present. The experimental data is discussed in light of our recent results on the γ-radiolysis of the analogous aqueous ZnO system.

2. Experimental

ZnO (99.9%, ~270 nm average particle diameter) was procured from Sigma Aldrich and used without further purification. The specific surface area (5.41 ± 0.10 m^2/g) was measured by the BET method using a Tristar II Surface Area Analyser. The crystal structure was determined by X-ray Diffraction using a Bruker D8 diffractometer and was found to be (0001) hexagonal wurtzite. Prior to irradiation, samples were baked at 400°C for a period of 24 h to remove adsorbed water and residual organic contaminants; the cleanliness of the samples was confirmed using Diffuse Reflectance Fourier Transform Spectroscopy (DRIFT). The temperature programmed desorption of water from the surface of the powder samples was used to determine at what point the oxide could be considered free of physisorbed water by tracking the reduction in the strength of the OH stretch between 3100-3700 cm^{-1} as the temperature increases. This was found to be above 400°C, however, the presence of chemisorbed species cannot be ruled out. Neither heat treatment or irradiation up to the maximum dose was observed to alter the particle size or crystal structure.

In order to prepare ~5.0 mL samples, the appropriate weight percent (wt%) of ZnO powder was mixed with the corresponding wt% of deionised H_2O (18.2 MΩ/cm) to make 60-90 wt% water slurries. The slurries were then introduced to a specially adapted glass sample cell which is coupled directly to the Gas Chromatograph (GC) and purged of air with Ar. Argon is the carrier gas of choice

for H_2 detection using a Thermal Conductivity Detector (TCD) due to the large difference in their thermal conductivities. A constant stream of N_2 is flown through the small volume between the end of the beam line and the sample cell to prevent the formation of O_3 from air radiolysis. A schematic diagram of the experimental setup is shown in Figure 1.

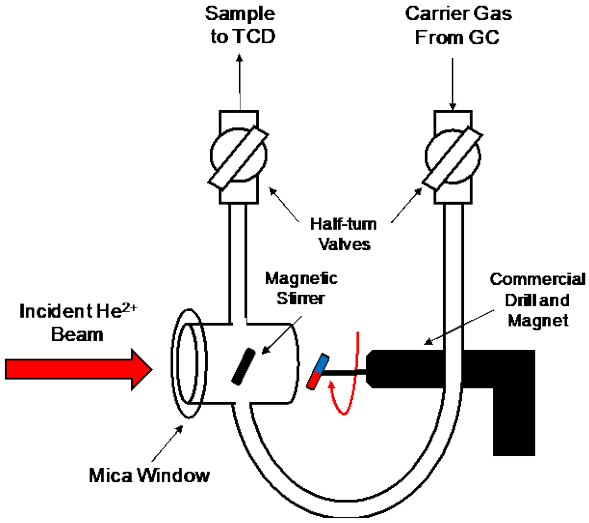

Figure 1 Schematic diagram of U-shaped sample cell with mica window of known density, thickness and composition used for ion beam irradiation. Gas Chromatography (GC) is coupled directly *via* haf-turn valves. 5.0 mL of the slurry sample is introduced to the sample cell and stirred at a high rate by a magnetic stirrer affixed to a commercial drill.

Irradiations were performed using 5.5 MeV He^{2+} ions produced using an NEC Van de Graff Tandem Pelletron 15SDH-4 accelerator employing a Toroidal Volume Ion Source (TORVIS) located at the Dalton Cumbrian Facility, The University of Manchester. The initial accelerator potential was set in order to ensure the ion beam had an energy of 5.5 MeV on the sample. The titanium exit window is 8 μm thick and has a density of 4.506 g cm^{-3}. There is a gap at the end of the beam line of 6.6 mm between the titanium exit window and mica window of the sample cell which is purged with N_2 gas, the density of which is 1.25×10^{-3} g cm^{-3}. The mica (K 9.81%, Al 20.3%, Si 21.13%, O 47.35%, H 0.45%, F 0.95%) window has a density of 2.82 g cm^{-3} with a thickness of between 2.12×10^{-3} cm and 2.85×10^{-3} cm depending on the sample cell in use. Energy will be lost due to the stopping power of each of these components, hence the initial beam energy was calculated using the TRIM (Transport of Ions in Matter) software package,[27] and was set to either 10.28 MeV or 10.86 MeV depending on the thickness of the mica window in use. The beam current incident on the sample was thus around 5.0 ±

0.1 nA with a beam diameter of approximately 3.0 mm. The dose was calculated by attaching a Keithley 6485 picoammeter directly to the sample cell and and measuring the accumulated charge as a function of time.

The oxide containing suspension is constantly stirred at a high rate using a magnetic stirrer mounted to a commercial drill as shown in Figure 1, with the aim to distribute reactive species in the sample homogeneously, giving reproducible results, and it further prevents the nanoparticles from settling.

The gases produced were analysed using a specially adapted SRI 8610C GC coupled to a TCD. Detection of gases by the TCD relies on the principle that the analyte gas has a significantly different thermal conductivity to the carrier gas, therefore, for H_2 sensitivity, the carrier gas of choice is Ar.[28,29] The sample cell is connected directly to the GC sample loop. Calibration of the GC was performed by injecting known amounts of pre-mixed 5% H_2 in Ar (from Scientific Gases Ltd.). The error associated with the measurements in the amount of gas measured is calculated to be 5.0% and considered to propagate throughout.

3. Results and Discussion

Radiation chemical yields are conventionally described by the G value, the number of molecules of a species produced, or consumed, per 100 eV of energy absorbed by the irradiated system. The G value for H_2 production from deaerated water by 5.5 MeV He^{2+} ions is ~1.20 molecules/100 eV.[30] In order to investigate the effect of the presence of the oxide on the yield of H_2 from water radiolysis, the 5.5 MeV He^{2+} irradiation of pure water was measured and this measurement was subsequently used as a benchmark, so deviation from this value can be attributed to the presence of the oxide.

At this point, it is worth pointing out that in the subsequent discussion, the absorbed energy is calculated with respect to mass the whole irradiated system such that any deviation in the $G(H_2)$ value from the value obtained for deaerated water radiolysis can be attributed to the presence of the oxide.[31] Using the same conditions throughout, the $G(H_2)$ value for pure water was determined to be 1.65 ± 0.13 molecules/100 eV, greater than the value reported by LaVerne *et al.* of 1.20 ± 0.12 molecules/100 eV.[30] This 25% discrepancy in $G(H_2)$ value for deaerated water radiolysis could have arisen from various sources. The most likely explanation is related to the energy

of the α-particles; uncertainties in the thickness of the titanium exit window of the beam line and thickness and composition the specific mica window used on each sample cell leads to differences between the calculated ion beam energy and the actual energy the sample receives, resulting in different radiolytic yields.

Due to the nature of the suspended solids within the samples, they must be stirred at a high rate to ensure the ZnO nanaoparticles do not settle and remain evenly dispersed throughout the solvent. In addition, the slurry is stirred at a high rate because, unlike γ-rays, the energy from ion irradiation is not necessarily distributed evenly throughout the sample. Due to the LET of the He^{2+} ion beam, a high concentration of ionised and excited species form in the radiation tracks at the point of beam entry into the sample, hence stirring is necessary to refresh the irradiation volume in order to ensure that the volume just behind the mica window is *not* over-exposed and receives a disproportionately high dose, but instead species become dispersed in the solution after irradiation, especially as the wt% of water decreases in the sample.

Figure 2 shows the production of H_2 for 20 wt% ZnO (5.41 m^2/g) in water (18.2 MΩ cm^{-1}). The radiolytic yield is expressed as the number of molecules and the absorbed energy is expressed in units of 100 eV, such that $G(H_2)$ values can be extracted directly from the slope of the linear best fit passing through the origin.

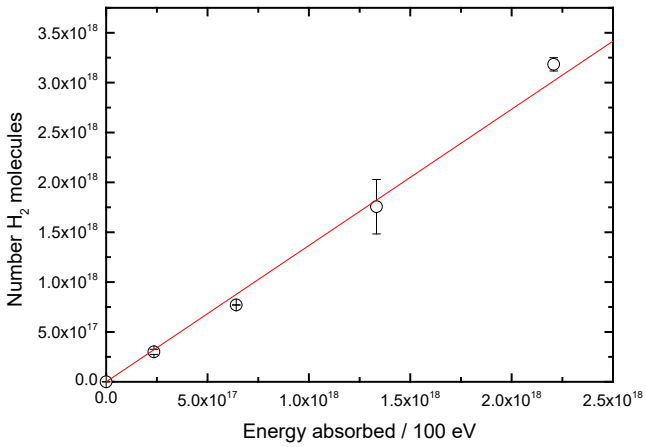

Figure 2 Number of molecules of H_2 produced as a function of energy absorbed for the 5.5 MeV He^{2+} irradiation of 20 wt% ZnO (5.41 m^2/g) in water (18.2 MΩ cm^{-1}). H_2 production appears linear up to the maximum dose delivered in this experiment. Each data point is an average of three measurements taken at the same absorbed dose.

Un-irradiated aqueous suspensions of ZnO did not yield any H_2 or O_2, indicating that gas production was indeed a radiation-induced process. The radiolytic production of H_2 is linear with respect to the absorbed energy, up to the maximum dose delivered in this series of experiments. Each point is an average of three measurements taken at the same dose and dose rate.

It is worth pointing out at this stage that in our previous work on the γ-ray radiolysis of water adsorbed on ZnO nanoparticles (i.e. in the solid phase, not slurries), we observed O_2 gas in comparable amounts to H_2.[26] However, O_2 was not observed in this series of experiments, most likely due to the experiments being performed in aqueous solutions, which significantly reduces the sensitivity towards O_2 gas as compared to detection of gas-phase O_2 in the vacuum above a solid phase as in our γ-radiation experiments.

The method displayed to extract $G(H_2)$ values, exemplified in Figure 2, is used for various concentrations of ZnO to evaluate the variation in $G(H_2)$ with the wt% of water. In order to account for the discrepancy in $G(H_2)$ observed between the experimental data obtained and the accepted literature data for deaerated water radiolysis, Figure 3 shows the G value as a fraction of the value obtained from deaerated water radiolysis, $G(H_2) = (G_{exp}(H_2) / 1.65) \times 1.20$ where $G_{exp}(H_2)$ are the experimentally obtained values.

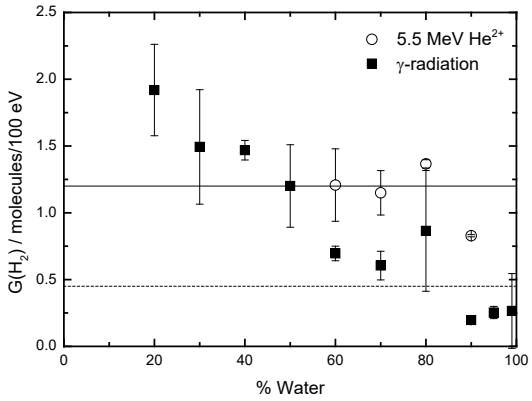

Figure 3 $G(H_2)$ values obtained from irradiation of ZnO (5.41 m^2/g) slurries from 60-90 wt% water by 5.5 MeV He^{2+} ions (open circles ○) and γ-rays (closed squares ■).[26] Due to the discrepancy between the literature and experimental $G(H_2)$ values for 5.5 MeV ion irradiation of deaerated water, yields are expressed here as a fraction of the experimental values obtained for deaerated water, i.e. $G(H_2) = (G_{exp}(H_2)/1.65)\times1.20$. The values expected for water with mMol concentrations of radical scavenger are shown for 5.5 MeV He^{2+} ions (solid lines) and γ–rays (dashed lines), respectively.

At 80 and 90 wt% water the solution is free flowing in nature, however, at 60 and 70 wt% the sample becomes much more like a paste and is difficult to stir. The large error associated with the data points at 60 and 70 wt% water in Figure 3 arises from this changing composition. Therefore, the investigation was limited to 60-90 wt% water as the sample becomes significantly harder to stir as the amount of ZnO increases. Because at lower wt% in water, the sample is less homogeneous in nature, even when stirred vigorously, and energy deposition into the sample cannot be assumed to be even. The diffusion of reactive species away from the radiation track may also be affected as the reactive species are more likely to interact with oxide particles as the wt% of water decreases due to the increased probability of radiolysis products encountering metal oxide particles.

The penetration depth of the ion beam into an aqueous sample of this nature is of the order of micrometres calculated using the SRIM (Stopping Range of Ions in Matter) software package.[27,32,33]

For the aqueous sample containing ZnO, the penetration depth was determined to be ~44 μm. If the sample was left un-agitated, the spot in contact with the mica window would become 'baked' (i.e. the oxide could be dried onto the sample cell window) as it would receive the entire dose of the irradiation. Therefore, to achieve roughly uniform irradiation and to avoid a small volume receiving a disproportionately high dose, there must be continuous, rapid mixing of the solution. This can be tested by varying the speed of the magnetic stirrer and observing the yield response. Once there is no further variation in yield with increased stirrer speed, the solution is considered to be mixed adequately to assume an even dose distribution.

The proximity of the G values to those observed for deaerated water indicate that there is little energy transfer occurring from the oxide to the solvating water. However, this does not explain the reduction in $G(H_2)$ observed at 90 wt% water.

Figure 3 also shows the $G(H_2)$ values for the γ-ray radiolysis of 20-98 wt% water. The error associated with the γ-ray experiments is smaller compared to He^{2+} irradiation, presumably due to the more even dispersion of radiation throughout the sample. The dashed line in Figure 3 displays the $G(H_2)$ value obtained from the γ-ray radiolysis of water containing mMol amounts of a radical scavenger such as a Br^- ions. Radical scavengers, in effect, protect H_2 being consumed by

preferentially reacting with the $OH^{\cdot}$ radical (the primary H_2 consuming species). For γ-radiolysis, this results in an increase in $G(H_2)$ from 0.20 (without scavenger) to a more realistic value of 0.45 molecules/100 eV with the radical scavenger. However, during heavy ion irradiation, this effect is not observed. Due to the significantly higher LET of heavy ions, far fewer OH radicals or hydrated electrons are formed from α-radiation compared to γ-rays, hence the Br^- ions have fewer species to react with, resulting in similar radiolytic yields in the absence or presence of bromides during α-irradiation (while yields for γ-irradiation differ far more depending on the presence or absence of scavengers).

Greater LET radiation results in greater radiolytic yields of H_2 as fewer radical species are produced per volume element, hence there are fewer H_2 consuming species present (i.e. fewer OH radicals). Therefore, it is expected that $G(H_2)$ value is greater for He^{2+} irradiation than γ-radiolysis. However, the $G(H_2)$ values were lower than one would expect if energy transfer from the ZnO particles into the adsorbed water was occurring as the maximum observed G value (1.36 molecules/100 eV) is close to the value observed for deaerated water radiolysis.

The reduction in G value at 90 wt% water may be due to the size of the nanoparticles used, in this case ~270 nm particle diameter. If the energy transfer is occurring from the oxide, excitons or excess electrons formed in large particles may not reach the interface before quenching. Alternatively, excited species formed away from oxide particles, at a diffusion controlled rate, may react with other radiolytic species before reaching an oxide particle for reaction, an effect observed in the radiolysis of water with silica (SiO_2) nanoparticles.[34] However, this does not explain the reduced $G(H_2)$ at 90 wt% water, nor can an explanation be offered for the increase in $G(H_2)$ from 70 to 80 wt% water. There is limited literature data on similar experiments with other oxides, but to overcome the aforementioned uncertainties in experimental data, and despite the experimental difficulties associated with α-irradiation, we would encourage more research into the α-radiation catalytic effects on water in the presence of metal oxides.[35,36,37]

4. Conclusions

We here describe the variation in radiolytic yields of H_2 from the irradiation of a range of aqueous suspensions of ZnO varying from 60 wt% to 90 wt% water. Radiolysis was induced using 5.5 MeV He^{2+} ions, and the gaseous products generated were analysed using an in-line gas chromatography setup.

The maximum $G(H_2)$ value observed was 1.36 molecules/100 eV however at 80 wt% water, while the G value was roughly the same as the value for deaerated water at 70 and 60 wt% water. $G(H_2)$ appeared to be lower than the G value for deaerated water at 90 wt% H_2O at 0.86 molecules/100 eV. H_2 yields were greater than those observed in the γ-ray radiolysis of 60-90 wt% water systems, which is expected due to the LET effect, but not as high as expected when compared with the value for α-particle radiolysis of pure water.

H_2 yields were roughly similar to pure water radiolysis at 60 and 70 wt% water indicating the same magnitude of G value enhancement does not occur with α-particles compared to γ-rays, however, this could be an LET effect. The production of O_2 was not observed in these experiments which is consistent with the γ-ray radiolysis of aqueous ZnO systems. That is not to say O_2 is not produced, but any molecular oxygen that may form could become solvated in the surrounding water.

Acknowledgement

J.S.S. thanks the UK National Nuclear Laboratory for funding through an EPSRC iCASE studentship. The authors thank Robin Orr and Howard Sims for helpful discussions.

Funding

This research was funded by EPSRC and the Dalton Cumbrian Facility project, a joint collaboration of the UK Nuclear Decommissioning Authority and The University of Manchester.

Reference

[1] Petrik, N. G.; Alexandrov, A. B.; Vall, A. I.; Interfacial Energy Transfer during Gamma Radiolysis of Water on the Surface of ZrO_2 and Some Other Oxides, *J. Phys. Chem. B*, **2001**, *105*, 5935-5944

[2] LaVerne, J. A.; Tandon, L.; H_2 Production in the Radiolysis of Water on CeO_2 and ZrO_2, *J. Phys. Chem. B,* **2002**, *106*, 380-386

[3] Sims, H. E.; Webb, K. J.; Brown, J.; Morris, J.; Taylor, J. R.; Hydrogen Yields from Water on the Surface of Plutonium Dioxide, *J. Nuc. Mater.*, **2013,** *437*, 359-364

[4] LaVerne, J. A.; Tandon, L.; H_2 Production in the Radiolysis of Water on UO_2 and Other Oxides, *J. Phys. Chem. B,* **2003**, *107*, 13623-13628

[5] LaVerne, J. A.; Tonnies, S. E.; H_2 Production in the Radiolysis of Aqueous SiO_2 Suspensions and Slurries, *J. Phys. Chem. B,* **2003**, *107*, 7277-7280

[6] Le Caër. S, Water Radiolysis: Influence of Oxide Surfaces on H_2 Production under Ionizing Radiation, *Water*, **2011**, *3*, 235-253

[7] Nakashima, M.; Aratono, Y.; Radiolytic Hydrogen Gas Formation from Water Adsorbed on Type A Zeolites, *Radiat. Phys. Chem.,* **1993**, *41*, 461-465

[8] Spinks, J. W. T.; Woods, R. J.; *An Introduction to Radiation Chemistry*, 3rd Edition, John Wiley & Sons, Inc, New York, **1964**, 39-77

[9] Burton, M.; Radiation Chemistry, *J. Phys. Chem.*, **1947**, *51*, 611-625

[10] Crumière, F.; Vandenborre, J.; Essehli, R.; Blain, G.; Barbet, J.; Fattahi, M.; LET Effects on the Hydrogen Production Induced by the Radiolysis of Pure Water, *Rad. Phys and Chem.,* **2013**, *82*, 74-79

[11] Appleby, A.; Schwarz, H. A.; Radical Yields in Water Irradiated by γ-rays and Heavy Ions, *J. Phys. Chem*, **1969**, *6*, 1937-1941

[12] Baldacchin, G.; Pulse Radiolysis in Water with Heavy-Ion Beams. A Short Review, *Rad. Phys. Chem.*, **2008**, *77*, 1218-1223

[13] Carrasco- Flores, E. A.; LaVerne, J. A.; Surface Species Produced in the Radiolysis of Zirconia Nanoparticles, *J. Chem. Phys.*, **2007**, *127*, 234703

[14] LaVerne, J. A.; Track Effects of Heavy Ions in Liquid Water, *Radiat. Res.*, **2000**, *153*, 487–496

[15] Burns, W. G.; Sims, H. E.; Effect of Radiation Type in Water Radiolysis, *J. Chem. Soc.,* Faraday Trans., **1981**, *1*, 28030-28132

[16] Georg. Rabe, J.; Rabe, B.; Allen, A. O.; Radiolysis in the Adsorbed State, *J. Am. Chem. Soc.,* **1964**, *86*, 3887–3888

[17] Allen, A.; Sutherland, B. J. W.; Radiolysis of Pentane in the Adsorbed State*, J. Am. Chem. Soc.,* **1961**, *83*, 1040–1047

[18] Petrik, N. G.; Alexandrov, A. B.; Vall, A. I.; Interfacial Energy Transfer during Gamma Radiolysis of Water on the Surface of ZrO_2 and Some Other Oxides, *J. Phys. Chem. B*, **2001**, *105*, 5935-5944

[19] Rowntree, P.; Parenteau, L.; Sanche, L.; Electron Stimulated Desorption via Dissociative Attachment in Amorphous H_2O, *J. Chem. Phys.,* **1991**, *94*, 8570-8576

[20] Bhargava Ram, N.; Krishnakumar, E.; Dissociative electron attachment to methane probed using velocity slice imaging, *Chem. Phys. Lett.,* **2011**, 22-27

[21] Flurin-A, S.; Water Chemistry in Boiling Water Reactors – A Leibstadt-Specific Overview, *CHIMIA International Journal for Chemistry*, **2005**, *59*, 923-928

[22] Puyane, R.; Effectiveness of Isotope Depleted ZnO to Minimize Radiation Build-up in Boiling Water Nuclear Reactors, *J. Mater. Process. Technol.,* **1996**, *56*, 863-872

[23] Debanath, M. K.; Karmakar, S.; Study of Blueshift of Optical Band Gap in Zinc Oxide (ZnO) Nanoparticles Prepared by Low-Temperature Wet Chemical Method, *Mater. Lett.,* **2013**, *111*, 116-119

[24] Sriyono, F.; Widodo, S.; Rina Sunaryo, G.; The effect of zinc injection on the increasing Inconel 600TT corrosion resistances, *J. Phys: Conf. Ser.,* **962**, 1-8

[25] Lv, J.; Li, X.; Defect Evolution in ZnO and its Effect on Radiation Tolerance, *Phys. Chem. Chem. Phys.,* **2018**, *20*, 11882-11887

[26] Southworth, J. S.; Koehler, S. P. K., Pimblott, S. M.; Gas Production from the Radiolysis of Water Adsorbed on ZnO Nanoparticles, *J. Phys. Chem. C,* **2018**, *112*, 25158-25164

[27] Ziegler, J. F.; Ziegler, M. D.; Biersack, J. P.; SRIM - The stopping and range of ions in matter, *Nucl. Instr. Meth. B,* **2010**, *268*, 1818-1823

[28] Johnston, H. L.; Grilly, E. R.; The Thermal Conductivites of Eight Common Gases between 80° and 380° K, *J. Chem. Phys.,* **1946**, *14*, 233-238

[29] Huber, M. L.; Harvey, A. H.; Thermal Conductivity of Gases, *CRC Handbook of Chemistry and Physics*, **2011**, *92*, 240-241

[30] Pimblott, S. M.; LaVerne, J. A.; Mozumder, A.; Monte Carlo Simulation Range and Energy Deposition by Electrons in Gaseous and Liquid Water, *J. Phys. Chem.,* **1996**, *100*, 8595-8606

[31] Spinks, J. W. T.; Woods, R. J.; *An Introduction to Radiation Chemistry*, 3rd Edition, John Wiley & Sons, Inc, New York, **1964**, 39-77

[32] Ziegler, J. F.; Ziegler, M. D.; Biersack, J. P.; SRIM - The stopping and range of ions in matter, *Nucl. Instr. Meth. B,* **2010**, *268*, 1818-1823

[33] P. Bauer, P.; Kastner, F.; Arnau, A.; Salin, A.; Fainstein, P. D.; Ponce V. H.; Echenique, P. M.; Stopping power of ions in materials, *Phys. Rev. Lett.* **1992**, *69*, 1137

[34] LaVerne, J. A.; Tonnies, S. E.; H_2 Production in the Radiolysis of Aqueous SiO_2 Suspensions and Slurries, *J. Phys. Chem. B,* **2003**, *107*, 7277-7280

[35] Rieff, S. C.; LaVerne, J. A.; Radiolysis of Water with Aluminum Oxide Surfaces, *Rad. Phys. Chem.,* **2017**, *131*, 46-50

[36] Rieff, S. C.; LaVerne, J. A.; Gamma and He Ion Radiolysis of Copper Oxides, *J. Phys. Chem. C*, **2015**, *119*, 8821-8828

[37] Rieff, S. C.; LaVerne, J. A.; Radiation Induced Changes to Iron Oxides, *J. Phys. Chem. B,* **2015**, *119*, 7358-7365